PROCEEDINGS OF THE WORLD CONFERENCE ON SHELL STRUCTURES
National Academy of Sciences

COMPARATIVE ANALYSES OF THIN PARABOLOIDAL SHELLS OF REVOLUTION UNDER GRAVITY LOAD

J. W. MAR
Associate Professor, MIT
F. Y. M. WAN
Lincoln Laboratory, MIT*

INTRODUCTION

The motivation for the work described in this paper is the quest for larger and more accurate reflecting surfaces. Radio astronomers and radar designers are continually pushing on to higher and higher frequencies. To the structural designers, this means the construction of reflectors on the order of 100 or more feet in diameter with the restriction that these reflectors cannot deviate more than several hundredths of an inch from the desired shape of a paraboloidal shell of revolution. This is a very stringent specification and requires a deflection analysis of the structure to an accuracy that is more difficult to attain than, for example, that for stresses necessary for the strength design.

The behavior of thin elastic shells under prescribed loading conditions has been the subject of numerous investigations. Through these investigations, the equations governing the shell behavior and the associated boundary conditions have been established; the conditions for membrane behavior, the extent of the edge zone effect, the applicability of shallow shell theory, and other characteristics of a thin elastic shell have become well understood. However, there is a considerable hiatus between the equations that govern the shell behavior and the numerical results that are necessary for engineering purposes. The reason, of course, is the inherent complexities of the equations and their solutions. In view of the time and labor involved, it is not practical for a designer to tackle anew the solutions of the shell equations whenever the feasibility of a new design is in doubt. We hope that the work described here will be of aid and comfort to the structural engineer who must bear the responsibility for the integrity of his design and who must, therefore, assign numbers to his answers.

The paraboloidal shell of revolution under gravity load has been analyzed in detail (within the framework of small deflection theory) by: 1. membrane theory, 2. shallow shell theory, 3. asymptotic integration of the usual two-dimensional shell equations, and 4. numerical integration of the same shell equations. Appropriate comparisons of the numerical results clearly delineate the meaning of membrane behavior, edge zone effect, and shallow shell behavior, expose the limitations of each method of analysis, and make explicit the behavior of the shell. There are a few surprises or effects that have not been predicted by previous investigations. However, the numerical results do permit quantitative determination of conclusions that heretofore were only known qualitatively.

Consideration will be confined to a simply supported, closed paraboloidal shell of revolution (homogeneous, isotropic, and with constant thickness), whose axis of revolution coincides with the direction of gravity. Restricted though this case may be, it does illustrate most of the properties exhibited by the shell. Paraboloidal shells oriented arbitrarily with respect to the gravity axis (i.e., without axi-symmetry) and with other com-

*Operated with support from U.S. Army, Navy, and Air Force

ABSTRACT

The deflections and stresses of paraboloidal shells of revolution under gravity load have been analyzed in detail by: 1. membrane theory, 2. shallow shell theory, 3. asymptotic integration of the shell equations, and 4. numerical integration of the same shell equations. Results of numerical calculations have been compiled in a form suitable for design. A description of these analyses for shells whose axis of revolution coincides with the direction of gravity is presented, and the characteristic behavior of the shells is discussed.

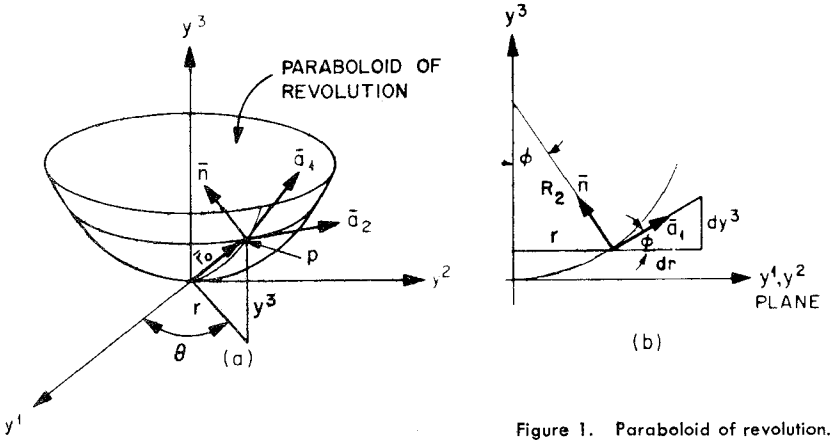

Figure 1. Paraboloid of revolution.

binations of edge conditions have also been investigated [1]; the results await future publication. Computer programs (written for the IBM 7090) which analyze paraboloidal shells in a manner described herein will be deposited in SHARE in the near future.

FORMULATION OF THE PROBLEM

The equation of the middle surface of a paraboloidal shell of revolution is

$$y^3 = \frac{r^2}{4f} \tag{1}$$

where f is the focal length of the paraboloid and r is the distance between the surface and the axis of revolution y^3 (Figure 1). Corresponding expressions for the relevant geometric quantities are

$$\begin{aligned} &A_1 = 2f\sqrt{1+\gamma^2}, \quad A_2 = 2f\gamma, \quad A_{12} = 0 \\ &R_1 = 2f(1+\gamma^2)^{3/2}, \; R_2 = 2f\sqrt{1+\gamma^2} \\ &\frac{1}{R_{12}} = 0 \end{aligned} \tag{2}$$

where

$$\gamma = \frac{r}{2f} = \frac{dy^3}{dr} = \tan\varphi$$

In the derivation of the above expressions, we have implicitly chosen the non-dimensional parameters γ and θ as the two middle surface coordinates ξ_1 and ξ_2. The corresponding base vectors $\vec{a_1}$, $\vec{a_2}$ and a third vector $\vec{n}$ defined by the cross product of $\vec{a_1}$ and $\vec{a_2}$ form an orthogonal system of shell coordinates. In the subsequent development, the subscripts 1 and 2 will be replaced by r and θ respectively wherever it seems more connotative.

The usual two-dimensional theory of thin elastic shells requires the satisfaction of the following equilibrium conditions by the stress resultants and bending moments.

$$\begin{aligned} &\frac{d(\gamma N_r)}{d\gamma} - N_\theta + \frac{\gamma}{1+\gamma^2} V_r = 2f\rho_0 h\gamma^2 \\ &\frac{d(\gamma V_r)}{d\gamma} + \frac{\gamma}{1+\gamma^2} N_r + \gamma N_\theta = 2f\rho_0 h\gamma \\ &\frac{d(\gamma M_r)}{d\gamma} - M_\theta - 2f\gamma\sqrt{1+\gamma^2}\, V_r = 0 \end{aligned} \tag{3}$$

where ρ_0 is the weight density of the shell.

If the displacements of the shell are small in comparison with the shell thickness, and if the transverse shear deformability is neglected, the strains of the shell can be related to the middle surface displacements and to the stress resultants and bending moments as follows

$$\epsilon_r = \bar{\epsilon}_r - z\chi_r \;, \quad \epsilon_\theta = \bar{\epsilon}_\theta - z\chi_\theta \tag{4}$$

where

$$\begin{aligned} \bar{\epsilon}_r &= \frac{1}{2f\sqrt{1+\gamma^2}} \frac{du_r}{d\gamma} - \frac{w}{2f[1+\gamma^2]^{3/2}} \\ &= \frac{N_r - \nu N_\theta}{Eh} \\ \bar{\epsilon}_\theta &= \frac{u_r}{2f\gamma\sqrt{1+\gamma^2}} - \frac{w}{2f\sqrt{1+\gamma^2}} \\ &= \frac{N_\theta - \nu N_r}{Eh} \end{aligned} \tag{5}$$

$$\chi_r = \frac{1}{2f\sqrt{1+\gamma^2}} \frac{d\theta_r}{d\gamma} = \frac{-(M_r - \nu M_\theta)}{D(1-\nu^2)}$$

$$\chi_\theta = \frac{\theta_r}{2f\gamma\sqrt{1+\gamma^2}} = \frac{-(M_\theta - \nu M_r)}{D(1-\nu^2)}$$

$$\theta_r = \frac{u_r}{2f[1+\gamma^2]^{3/2}} + \frac{1}{2f\sqrt{1+\gamma^2}} \frac{dw}{d\gamma} \tag{6}$$

The middle surface displacement components u_r and w are in turn related to the displacement components of the shell U_r and W by

$$U_r = u_r - z\theta_r \;, \quad W = w \tag{7}$$

It is to be understood that the system of shell equations (3), (5), and (6) is defined over the interval $0 \leq \gamma_l \leq \gamma \leq \gamma_u$ where the corresponding r_l and r_u are the lower and upper edge of the shell respectively ($r_l = 0$ in the present consideration as the shell is closed at the apex). These equations are supplemented by the simply supported edge condition at γ_u, i.e.,

$$w\,(\gamma_u) = u_r\,(\gamma_u) = M_r\,(\gamma_u) = 0 \tag{8}$$

and the condition of finiteness at the apex of the shell.

MEMBRANE BEHAVIOR

Under the proper circumstances, the paraboloidal shell will prefer to carry the applied loads by the development of the stress resultants N_r and N_θ rather than by the development of the transverse shear resultant V_r

and bending moments M_r and M_θ. The investigation of the shell behavior can be simplified considerably if we assume χ_r and χ_θ (and consequently M_r, M_θ and V_r) to be absent throughout the shell. In other words, the shell is assumed to have no bending stiffness. Such behavior of the shell is commonly called the membrane behavior although the term "momentless" behavior is more connotative. The so-called membrane equations are easily obtained by omitting the M_r, M_θ and V_r terms from the equations of equilibrium.

$$\begin{aligned} &\frac{d(\gamma N_r)}{d\gamma} - N_\theta = 2f\rho_0 h\gamma^2 \\ &\frac{N_r}{1+\gamma^2} + N_\theta = 2f\rho_0 h \end{aligned} \tag{9}$$

This system of equations can now be solved for N_r and N_θ without any reference to the strain-displacement relations.

It should be observed that the system of equations for determining the displacements u_r and w is also equivalent to a 1st order differential equation (6). In other words, the membrane behavior is governed by a 2nd order system, and only one condition can be prescribed at each edge of the shell. It is clear from the equations themselves that one of these conditions must be given in terms of the displacements and that the remaining condition can be given either in terms of the displacements or the stress resultants, with the restriction that the shell may neither be constrained in the normal direction nor experience a transverse edge load [2], [3].

In our investigations, the shell is to be constrained in the tangential direction so that $u_r(\gamma_u) = 0$ and the condition of finiteness will be imposed upon N_r at the apex. Thus we have

$$\begin{aligned} N_r &= \frac{2f\rho_0 h}{3\gamma^2}\left[(1+\gamma^2)^{3/2} + C_1\right] \\ N_\theta &= 2f\rho_0 h\left[1 - \frac{(1+\gamma^2)^{3/2} + C_1}{3\gamma^2\sqrt{1+\gamma^2}}\right] \end{aligned} \tag{10}$$

where $C_1 = -1$. The displacement components u_r and w can now be obtained from (6).

$$\begin{aligned} u_r = \frac{4f^2\rho_0}{3E\sqrt{1+\gamma^2}}\Bigg\{&(1+\nu)\gamma\log_e\gamma - \frac{(1+\nu)}{\gamma} + \left(\frac{3-\nu}{2}\right)\gamma^3 \\ &+ \frac{\gamma^5}{4} + C_1\left[\gamma\sqrt{1+\gamma^2} - \frac{(1+\nu)\sqrt{1+\gamma^2}}{\gamma}\right. \\ &\left. - (1+\nu)\gamma\log_e\left(\frac{1+\sqrt{1+\gamma^2}}{\gamma}\right)\right] + C_2\gamma\Bigg\} \end{aligned} \tag{11}$$

$$\begin{aligned} w = \frac{4f^2\rho_0}{3E\sqrt{1+\gamma^2}}\Bigg\{&(1+\nu)\log_e\gamma - \frac{(1+\nu)}{\gamma^2} + \frac{(3-\nu)}{2}\gamma^2 \\ &+ \frac{\gamma^4}{4} + [1+\gamma^2]\left[2(\nu-1) + \frac{(1+\nu)}{\gamma^2} + \nu\gamma^2\right] \\ &+ C_1(1+\nu)\left[\sqrt{1+\gamma^2} - \log_e\left(\frac{1+\sqrt{1+\gamma^2}}{\gamma}\right)\right] + C_2\Bigg\} \end{aligned}$$

where C_2 is such that $u_r(\gamma_u) = 0$.

SHALLOW SHELL BEHAVIOR

A paraboloidal shell of revolution is considered shallow if

$$\left(\frac{dy^3}{dr}\right)^2 = \gamma^2 \ll 1 \tag{12}$$

so that

$$1 + \gamma^2 \cong 1$$

It can be shown [1] that if the approximation (12) is applied consistently, the system of shell equations can, without additional assumptions,[1] be reduced to

$$\begin{aligned} &-D\nabla^2\nabla^2 w + 2f\nabla^2 F = (2f)^4\rho_0 h \\ &A\nabla^2\nabla^2 F + 2f\nabla^2 w = -A(1-\nu)\,4f^3\rho_0 h \end{aligned} \tag{13}$$

where

$$\nabla^2(\ ) = \frac{d^2(\ )}{d\gamma^2} + \frac{1}{\gamma}\frac{d(\ )}{d\gamma} \quad , \quad A = \frac{1}{Eh}$$

F is a stress function from which N_r and N_θ are derivable.

$$N_r = \frac{1}{4f^2}\left(\frac{1}{\gamma}\frac{dF}{d\gamma}\right) \quad , \quad N_\theta = \frac{1}{4f^2}\left(\frac{d^2F}{d\gamma^2}\right) \tag{14}$$

we have also

$$V_r = \frac{-D}{8f^3}\frac{d(\nabla^2 w)}{d\gamma} \quad , \quad u_r = \gamma\,(2f\bar{\epsilon}_\theta + w)$$

[1] In order to arrive at an equivalent set of equations for an asymmetrically loaded shell, it is necessary to impose additional assumptions on the transverse shear resultants and the bending moments [4].

$$M_r = \frac{-D}{4f^2}\left(\frac{d^2w}{d\gamma^2} + \frac{\nu}{\gamma}\frac{dw}{d\gamma}\right) \quad , \quad M_\theta = \frac{-D}{4f^2}\left(\nu\frac{d^2w}{d\gamma^2} + \frac{1}{\gamma}\frac{dw}{d\gamma}\right) \tag{15}$$

The solutions to the system (13) and the corresponding stress resultants, tangential displacement component, and bending moments are

$$w = K_3 + K_1\,ber(k\gamma) + K_2\,bei(k\gamma) + K_4\,ker(k\gamma) + K_5\,kei(k\gamma) - \frac{4f^2\rho_0(1-\nu)}{E}\frac{\gamma^2}{2}$$

$$F = \frac{Eh^2}{\sqrt{12(1-\nu^2)}}[-K_1\,bei + K_2\,ber - K_4\,kei + K_5\,ker + K_6\log_e(k\gamma)] + \frac{f\rho_0 h}{2}(2f\gamma)^2$$

$$N_r = \frac{Eh}{2fk\gamma}\left[-K_1\,bei' + K_2\,ber' - K_4\,kei' + K_5\,ker' + \frac{K_6}{(k\gamma)}\right] + f\rho_0 h$$

$$N_\theta = \frac{-Eh}{2f}\left(K_1\,bei'' - K_2\,ber'' + K_4\,kei'' - K_5\,ker'' + \frac{K_6}{(k\gamma)^2}\right) + f\rho_0 h$$

$$V_r = -Dk^3(-K_1\,bei' + K_2\,ber' - K_4\,kei' + K_5\,ker')$$

$$M_r = -Dk^2\left[K_1\left(ber'' + \frac{\nu\,ber'}{k\gamma}\right) + K_2\left(bei'' + \frac{\nu\,bei'}{k\gamma}\right) + K_4\left(ker'' + \frac{\nu\,ker'}{k\gamma}\right)\right.$$
$$\left. + K_5\left(kei'' + \frac{\nu\,kei'}{k\gamma}\right)\right] + \frac{\rho_0 h^3}{12} \tag{16}$$

$$M_\theta = -Dk^2\left[K_1\left(\nu\,ber'' + \frac{ber'}{k\gamma}\right) + K_2\left(\nu\,bei'' + \frac{bei'}{k\gamma}\right) + K_4\left(\nu\,ker'' + \frac{ker'}{k\gamma}\right)\right.$$
$$\left. + K_5\left(\nu\,kei'' + \frac{kei'}{k\gamma}\right)\right] + \frac{\rho_0 h^3}{12}$$

$$u_r = \frac{1+\nu}{k}\left(K_1\,bei' - K_2\,ber' + K_4\,kei' - K_5\,ker' + \frac{K_3 k\gamma}{1+\nu} - \frac{K_6}{k\gamma}\right) + \frac{(1-\nu)f\rho_0}{E}(2f\gamma)$$

where

$$k^4 = 12\left(1-\nu^2\right)\left(\frac{2f}{h}\right)^2, \quad (\,)' = \frac{d(\,)}{d(k\gamma)}$$

$$I_0(\sqrt{i}\,k\gamma) = ber(k\gamma) + i\,bei(k\gamma) \quad , \quad K_0(\sqrt{i}\,k\gamma) = ker(k\gamma) + i\,kei(k\gamma)$$

K_i, $i = 1, 2, \ldots, 6$, are constants of integration. The condition of finiteness can be met by setting K_4, K_5, and K_6 equal to zero and the remaining constants can be determined by the simply supported edge condition (8). The portion of (16) which corresponds to the homogeneous solutions of (13) was first obtained by E. Reissner [5].

ASYMPTOTIC INTEGRATION

An equivalent form of the shell equations (3), (5), and (6) is the 4th order system [6], [7]

$$\frac{d^2\theta_r}{d\gamma^2} + \frac{1}{\gamma(1+\gamma^2)}\frac{d\theta_r}{d\gamma} - \left(\frac{1}{\gamma^2} + \frac{\nu}{1+\gamma^2}\right)\theta_r + \frac{2f\sqrt{1+\gamma^2}}{D}U = 0$$

$$\frac{d^2U}{d\gamma^2} + \frac{1}{\gamma(1+\gamma^2)}\frac{dU}{d\gamma} - \left(\frac{1}{\gamma^2} - \frac{\nu}{1+\gamma^2}\right)U - 2fEh\sqrt{1+\gamma^2}\,\theta_r = \theta_0 \tag{17}$$

where

$$\theta_0 = -\frac{4f^2\rho_0 h\gamma\sqrt{1+\gamma^2}}{3}[(1+3\nu) + C_1(1+\gamma^2)^{-3/2}]$$

$$U = 2f\sqrt{1+\gamma^2}\,V_r$$

In terms of U and θ_r, the relevant stress resultants, bending moments, and displacement components are

$$N_r = \frac{-V_r}{\gamma} + V_0 \ , \quad N_\theta = -\left(\frac{1}{2f\sqrt{1+\gamma^2}}\frac{dU}{d\gamma} + \frac{V_0}{1+\gamma^2} - 2f\rho_0 h\right)$$

$$M_r = \frac{-D}{2f\sqrt{1+\gamma^2}}\left(\frac{d\theta_r}{d\gamma} + \frac{\nu}{\gamma}\theta_r\right)$$

$$M_\theta = \frac{-D}{2f\sqrt{1+\gamma^2}}\left(\nu\frac{d\theta_r}{d\gamma} + \frac{\theta_r}{\gamma}\right) \tag{18}$$

$$w = \frac{2f}{\sqrt{1+\gamma^2}}\int[(1+\gamma^2)\theta_r - \gamma\bar{\epsilon}_\theta]d\gamma$$

$$u_r = \gamma w + u_h\sqrt{1+\gamma^2} = \gamma(2f\,\bar{\epsilon}_\theta\sqrt{1+\gamma^2} + w)$$

where

$$V_0 = \frac{2f\rho_0 h\sqrt{1+\gamma^2}}{3\gamma^2}[(1+\gamma^2)^{3/2} + C_1]$$

and u_h is the displacement in the radial direction. The system (17) can be reduced to a single 4th order differential equation in θ_r.

$$L\theta_r + 12(1-\nu^2)\left(\frac{2f}{h}\right)^2(1+\gamma^2)\theta_r = -\frac{2f\sqrt{1+\gamma^2}}{D}\theta_0 \tag{19}$$

where L is a 4th order linear differential operator. For a thin paraboloidal shell of revolution, $(2f/h) \gg 1$, an asymptotic expansion of the solution in powers of $(h/2f)^{1/2}$ is appropriate. Retaining only the leading term of the corresponding expansions and observing that the loading intensity does not vary appreciably over a distance of the order $(2fh)^{1/2}$, we have the following expressions for the quantities of interest

$$\theta_r = F_0[e^\psi(C_3\cos\psi + C_4\sin\psi) + e^{-\psi}(C_5\cos\psi + C_6\sin\psi)]$$

$$V_r = \frac{Eh^2}{4fm^2}\frac{F_0}{\sqrt{1+\gamma^2}}[e^\psi(C_3\sin\psi - C_4\cos\psi) - e^{-\psi}(C_5\sin\psi - C_6\cos\psi)]$$

$$N_r = \frac{-V_r}{\gamma} + \frac{2f\rho_0 h\sqrt{1+\gamma^2}}{3\gamma^2}[(1+\gamma^2)^{3/2} + C_1]$$

$$N_\theta = \frac{-Eh}{2m}\sqrt{\frac{h}{f}}\frac{F_0}{\sqrt[4]{1+\gamma^2}}\left\{e^\psi\left[C_3\sin\left(\psi+\frac{\pi}{4}\right) - C_4\cos\left(\psi+\frac{\pi}{4}\right)\right] + e^{-\psi}\left[C_5\sin\left(\psi-\frac{\pi}{4}\right) - C_6\cos\left(\psi-\frac{\pi}{4}\right)\right]\right\} + 2f\rho_0 h\left[1 - \frac{(1+\gamma^2)^{3/2} + C_1}{3\gamma^2\sqrt{1+\gamma^2}}\right] \tag{20}$$

$$M_r = \frac{-Eh^2}{4m^3}\sqrt{\frac{h}{f}}\frac{F_0}{\sqrt[4]{1+\gamma^2}}\left\{e^\psi\left[C_3\cos\left(\psi+\frac{\pi}{4}\right) + C_4\sin\left(\psi+\frac{\pi}{4}\right)\right] - e^{-\psi}\left[C_5\cos\left(\psi-\frac{\pi}{4}\right) + C_6\sin\left(\psi-\frac{\pi}{4}\right)\right]\right\}$$

$$M_\theta = \nu M_r \ , \quad u_r = u_m$$

$$w = \frac{\sqrt{fh}}{m}F_0\sqrt[4]{1+\gamma^2}\left\{e^\psi\left[C_3\sin\left(\psi+\frac{\pi}{4}\right) - C_4\cos\left(\psi+\frac{\pi}{4}\right)\right] + e^{-\psi}\left[C_5\sin\left(\psi-\frac{\pi}{4}\right) - C_6\cos\left(\psi-\frac{\pi}{4}\right)\right]\right\} + w_m$$

where

$$\psi = m\sqrt{\frac{2f}{h}}\int\sqrt[4]{1+\gamma^2}\,d\gamma \ , \quad F_0 = \frac{(1+\gamma^2)^{1/8}}{h\sqrt{\gamma}\,\sqrt[4]{2fh}} \ , \quad m = \sqrt[4]{3(1-\nu^2)}$$

u_m and w_m are given by the first and the second equations of (11), respectively. C_i, $i = 1, \ldots, 6$, are constants of integration.

The retention of the leading term in the homogeneous development for u_r (i.e., $u_r - u_m$) would necessitate the ascertainment of the second term in the expansions for V_r and θ_r, while neglecting the difference be-

tween u_r and u_m is equivalent to omitting terms of the order $u_m\ (h/2f)^{1/2}$. In the development above, a more consistent derivation of $u_r = u_m$ (up to an error of the order $(h/2f)^{1/2}$) would be to consider u_h and u_v, the axial displacement (which are of the same order in $(h/2f)^{1/2}$) instead of u_r and w. The solutions which are finite at the apex correspond to those obtained by setting $C_5 = C_6 = 0$ and $C_1 = -1$ in the above expressions. The remaining constants can be determined by the simply supported edge condition (8). The above results are essentially those derived by F. B. Hildebrand [8]. Note that we may arrive at the same results if we first express the equations of equilibrium for the stress resultants in terms of the displacement components, and then apply the technique of asymptotic integration to the resulting equations. The latter approach is also suitable for the asymptotic solutions to shells which are not loaded axisymmetrically.

NUMERICAL INTEGRATION

The differential equations (17) can be converted into finite difference equations by Stirling's interpolation formula truncated after the second difference.

$$\begin{aligned} &a_1^i\theta_r^{i+1} + a_2^i\theta_r^i + a_3^i\theta_r^{i-1} + a_4^iU^i = 0 \\ &a_1^iU^{i+1} + a_5^iU^i + a_3^iU^{i-1} + a_6^i\theta_r^i = \theta^i \end{aligned} \tag{21}$$

where

$$a_1^i = \gamma_i^2(1 + \gamma_i^2) + \delta_i\gamma_i$$

$$a_2^i = -\{\delta_i^2[1 + (1 + \nu)\gamma_i^2] + 2\gamma_i^2(1 + \gamma_i^2)\}$$

$$a_3^i = \gamma_i^2(1 + \gamma_i^2) - \delta_i\gamma_i$$

$$a_5^i = -\{\delta_i^2[1 + (1 - \nu)\gamma_i^2] + 2\gamma_i^2(1 + \gamma_i^2)\}$$

$$a_4^i = \frac{2f\gamma_i^2\delta_i^2(1 + \gamma_i^2)^{3/2}}{D}$$

$$a_6^i = -2fEh\gamma_i^2\delta_i^2(1 + \gamma_i^2)^{3/2}$$

$$\delta_i = \begin{cases} \frac{1}{2}(\gamma_{i+1} - \gamma_{i-1}), & 1 < i < m \\ (\gamma_{i+1} - \gamma_i), & i = 1 \\ (\gamma_i - \gamma_{i-1}), & i = m \end{cases}$$

$$\theta^i = \theta_0^i\delta_i^2\gamma_i^2(1 + \gamma_i^2)$$

and if X is a function of γ, the $X^i = X\ (\gamma_i)$.

Consider m discrete points in the interval $0 \leq \gamma_l \leq \gamma \leq \gamma_u$ (end points included). There are two equations of the form (21) for each point γ_i save $\gamma_l = 0$, for we can deduce from (17) that at the apex $U = \theta_r = 0$. Thus, there are $2(m\text{-}1)$ equations for the $2m$ unknowns $U^2, \ldots, U^{m+1}$ and $\theta_r^2, \ldots, \theta_r^{m+1}$. At the simply supported edge, we have

$$\frac{d\theta_r}{d\gamma} + \frac{\nu\theta_r}{\gamma} = 0\ , \qquad \frac{dU}{d\gamma} - \frac{\nu U}{\gamma} = -2f\sqrt{1 + \gamma^2}\left[V_0\left(\nu + \frac{1}{1 + \gamma^2}\right) - 2f\rho_0 h\right] \tag{22}$$

(22) may be used to express U^{m+1} and θ_r^{m+1} in terms of U^m, U^{m-1}, θ_r^m, and θ_r^{m-1} and thus reduces the number of unknowns by two to $2(m-1)$. A solution to the resulting set of simultaneous algebraic equations for U^i and θ^i_r, $i = 2, \ldots, m$, is now accessible by the usual method of matrix inversion or relaxation. Again, the relevant stress resultants, bending moments, and displacements can be obtained from U^i and θ^i_r by way of (18) where the differential and integral relations are replaced by the appropriate algebraic relations.

COMPUTATIONS

Computer programs have been written to carry out the necessary calculations for the four methods of analysis discussed above. In each of these programs, the inputs are the parameters which describe the geometry of the shell (h, f, r_l, and r_u), the properties of the material (E and ν), and the load (ρ_o). We may choose the edge condition to be simply supported or clamped. If the shell is not closed at the apex, any combination of these conditions can be prescribed. We also have the additional option of a free edge for one of the edges while the other is simply supported or clamped. The main outputs of these programs are the stress resultants, the bending moments, and the displacements, at the requested points on the shell. Except for the case of numerical integration, the calculations amount to first solving for the constants of integration according to the choice of boundary conditions and then using these constants to generate the desired information. We may mention that in the case of asymptotic integration, the results are erroneous in the vicinity of the apex of the shell where the asymptotic solutions cease to be meaningful. However, since the behavior of the shell at the apex can be deduced from the shell equations, the behavior

near the apex can be obtained, to a good approximation, by interpolation. A rigorous asymptotic solution can be valid near and at the apex [13].

In the analysis of the shell by numerical integration, the solution to the set of simultaneous algebraic equations is obtained by matrix inversion. For the sake of economy in computer time and simplicity in programming, the matrix elements are assumed to be stored in the core. This imposes a limitation on the size of the matrix which, in turn, means a possible sacrifice of accuracy. However, it is found that the difference (in θ_r and U) between using three-quarters and full capacity of the computer is about 6 per cent of the latter for $\gamma_{ii} < 1$ (3 per cent for $\gamma_{ii} \leq 0.6$). This implies that either the convergence of the numerical integration procedure is extremely slow or the limitation imposed on the size of the matrix is not a severe handicap for $\gamma_{ii} < 1$. A close examination of the results obtained by the different methods of analysis seems to favor the second possibility. Note that if integration is performed for (19) instead of (17), the storage requirement may be reduced by half. But the latter alternative yields reasonable results only for very coarse partitions of the interval $\gamma_i \leq \gamma \leq \gamma_{ii}$ (i.e., δ_i is not too small). This is not surprising for (19) is more sensitive to round-offs than (17). Since in actual design γ_{ii} is usually smaller than unity, the capacity of the computer is rarely taxed in the integration of (17), and we shall not pursue the integration of (19) here. A comparison and detailed discussion of the two integration procedures and the precise meaning of the above statements can be found in [1].

To compute the normal displacements in the same analysis, we can apply the trapezoidal rule (or other quadrature formula) to the integral for w in (18). As an alternative, the matrix inversion technique used above can be applied to the difference equations corresponding to

$$\frac{d^2w}{d\gamma^2} + \frac{2\gamma}{1+\gamma^2}\frac{dw}{d\gamma} + \frac{w}{1+\gamma^2} = 2f\left[(1+\gamma^2)\frac{d\theta_r}{d\gamma} + 3\gamma\theta_r - \bar{\epsilon}_r\right] \quad (23)$$

(23) is obtained by an appropriate combination of the last equation of (6) and the first equation of (5). Indirect though it may be, the latter approach has certain computational advantages when the difference between γ_{ii} and γ_i is small (Figure 2). In either case, additional error due both to round-off and truncation is introduced. Hence, the discrepancy between the displacement components obtained by numerical integration and those by other analyses is expected to be larger than the discrepancy in the stress resultants and bending moments. Calculations show that, for relatively deep shells ($\gamma_{ii} > 0.5$), the tangential displacements obtained in the analyses by numerical integration are erroneous. Fortunately, u_r is usually an order of magnitude smaller than w for $\gamma_{ii} \leq 1$; therefore, its contribution to the total displacement of the shell is negligible, and we shall omit further consideration of u_r hereafter.

EXPLANATION OF FIGURES AND TABLES

In presenting some of the numerical results, we have worked with the non-dimensionalized quantities

$$N_r^* = \frac{N_r}{2f\rho_0 h}, \qquad N_\theta^* = \frac{N_\theta}{2f\rho_0 h}, \qquad V_r^* = \frac{V_r}{\rho_0 h\sqrt{2fh}}$$

$$M_r^* = \frac{M_r}{2f\rho_0 h^2}, \qquad M_\theta^* = \frac{M_\theta}{2f\rho_0 h^2}, \qquad \theta_r^* = \frac{E\theta_r}{2f\rho_0}\sqrt{\frac{h}{2f}} \quad (24)$$

$$w^* = \frac{Ew}{4f^2\rho_0}$$

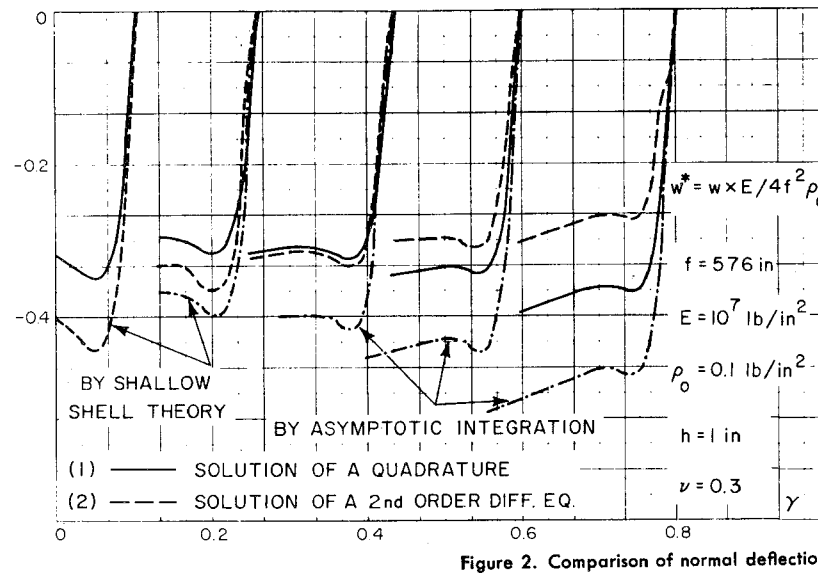

Figure 2. Comparison of normal deflection.

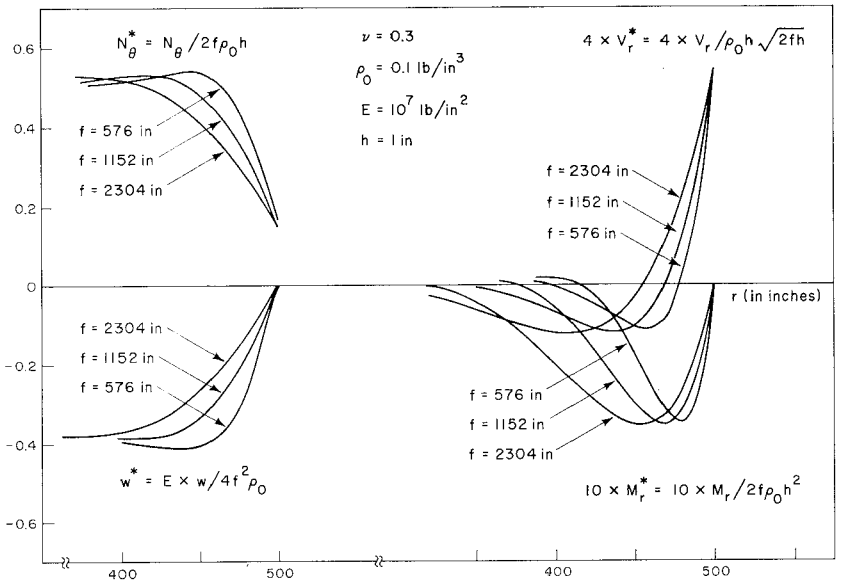

Figure 3. Edge effect vs focal length.

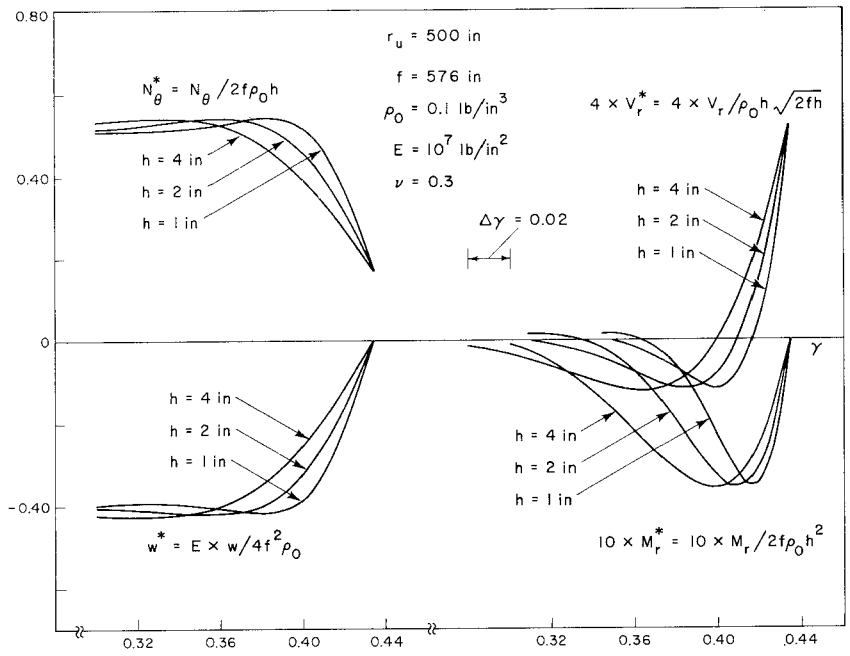

Figure 4. Edge effect vs shell thickness.

The normalizing factors are somewhat arbitrary for all except the membrane behavior in which special case the stress resultants and displacements can be scaled according to $2f\rho_0 h$ and $4f^2\rho_0/E$. In the other cases, the non-dimensionalizing factors, while having some degree of analytical justification as true scale factors, are used mainly for ease of presenting the results.

The computational errors in w^* associated with the numerical integration procedures are shown in Figure 2 for five different size shells (γ_u = 0.104, 0.260, 0.434, 0.600, 0.800). For the two smallest shells, the numerical integration of equations (18) (solution of a quadrature) and (24) (solution of a 2nd order differential equation) are compared to the results of shallow shell theory. For the other three, the results are compared with the solutions by asymptotic integration.

The widths of the zone in which bending of the shell is significant are shown in Figure 3 for shells of three different focal lengths by the variations of N_θ^*, w^*, V_r^*, and M_r^* near the simply supported edge. Note that the outer radii of the shells are 500 in. in each case and that the abscissa is r rather than γ.

Figure 4 makes the same comparisons as Figure 3 except that the shell thickness is varied rather than focal length.

The stress resultant N_θ^* and normal displacement w^* as computed by: 1. asymptotic integration, 2. shallow shell, 3. numerical integration, and 4. membrane methods are compared for five different size shells (γ_u = 0.104, 0.260, 0.347, 0.434, 0.521) in Figure 5. A single curve marked, for example, (1), (2), (3) means that these three methods produce essentially the same results in that region of γ.

Figure 6 is a companion to Figure 5 except that the quantities being compared are V_r^* and M_r^*. Note that the ordinate scales for V_r^* and M_r^* are different.

The comparisons made in Figure 5 are extended to four larger shells (γ_u = 0.60, 0.80, 1.00, 1.20) in Figure 7.

In Figure 8, the comparisons made in Figure 6 are extended to the four larger shells of Figure 7. Note again the different ordinate scales for V_r^* and M_r^*.

Representative numerical results for a shell with γ_u = 0.260 are tabulated in Table I for the various methods of solution. These are the numbers used for plotting the second (from the left) set of curves in Figures 5 and 6.

The numerical results used for plotting the last (from the left) set of curves (γ_u = 0.521) in Figures 5 and 6 are tabulated in Table II.

The numerical results used for plotting the third set (from the left) of curves (γ_u = 1.00) shown in Figures 7 and 8 are tabulated in Table III.

DISCUSSION OF RESULTS

Comparisons of the numerical results

Table I: **Comparison of Results**

$10 \times M_r^* = 10 \times M_r/2f\rho_0h^2$ | $10 \times M_\theta^* = 10 \times M_\theta/2f\rho_0h^2$

γ	Mem.	S.S.	A.I.	N.I.	Mem.	S.S.	A.I.	N.I.
0.137		0.0063	0.0043	0.0049		0.0025	0.0010	0.0012
0.143		0.0158	0.0070	0.0077		0.0037	0.0019	0.0023
0.156		0.0161	0.0135	0.0143		0.0066	0.0038	0.0050
0.169		0.0203	0.0179	0.0186		0.0089	0.0051	0.0070
0.186		0.0067	0.0072	0.0066		0.0058	0.0019	0.0042
0.189		−0.0008	0.0008	−0.0003		0.0035	0.0000	0.0021
0.192		−0.0106	−0.0077	−0.0093		0.0004	−0.0025	−0.0006
0.199		−0.0379	−0.0319	−0.0346		−0.0086	−0.0098	−0.0089
0.208		−0.1013	−0.0888	−0.0937		−0.0307	−0.0268	−0.0287
0.218		−0.1913	−0.1709	−0.1781		−0.0635	−0.0515	−0.0580
0.231		−0.3269	−0.3057	−0.3061		−0.1169	−0.0893	−0.1053
0.244		−0.3827	−0.3521	−0.4148		−0.1501	−0.1058	−0.1332
0.257		−0.1431	−0.1329	−0.1351		−0.0896	−0.0401	−0.0739

$N_r^* = N_r/2f\rho_0h$ | $N_\theta^* = N_\theta/2f\rho_0h$

γ	Mem.	S.S.	A.I.	N.I.	Mem.	S.S.	A.I.	N.I.
0.020	0.5001	0.5000	0.5001	0.5001	0.5001	0.5000	0.5001	0.5001
0.059	0.5013	0.5000	0.5013	0.5013	0.5004	0.5001	0.5005	0.5005
0.111	0.5046	0.4999	0.5045	0.5045	0.5015	0.4992	0.5008	0.5007
0.140	0.5073	0.4997	0.5071	0.5071	0.5024	0.4988	0.5011	0.5011
0.179	0.5120	0.5004	0.5123	0.5122	0.5039	0.5120	0.5144	0.5150
0.205	0.5157	0.5031	0.5184	0.5179	0.5051	0.5276	0.5314	0.5316
0.221	0.5183	0.5045	0.5223	0.5215	0.5059	0.5084	0.5165	0.5152
0.238	0.5211	0.5022	0.5231	0.5228	0.5067	0.4183	0.4354	0.4322
0.251	0.5235	0.4943	0.5184	0.5197	0.5075	0.2692	0.2970	0.2929
0.260	0.5253	0.4831	0.5102	0.5138	0.5078	0.1212	0.1576	0.1541

$w^* = Ew/4f^2\rho_0$ | $V_r^* = V_r/\rho_0h\sqrt{2fh}$

γ	Mem.	S.S.	A.I.	N.I.	γ	S.S.	A.I.	N.I.
0.020	−0.3734	−0.3721	−0.3733	−0.2984	0.179	−0.0027	−0.0021	−0.0017
0.143	−0.3700	−0.3778	−0.3689	−0.2947	0.192	−0.0101	−0.0086	−0.0053
0.199	−0.3669	−0.4138	−0.3914	−0.3142	0.205	−0.0213	−0.0186	−0.0149
0.205	−0.3665	−0.4174	−0.3934	−0.3162	0.218	−0.0321	−0.0284	−0.0228
0.218	−0.3655	−0.4093	−0.3835	−0.3092	0.225	−0.0338	−0.0302	−0.0243
0.231	−0.3646	−0.3605	−0.3363	−0.2722	0.231	−0.0301	−0.0271	−0.0220
0.241	−0.3638	−0.2809	−0.2613	−0.2124	0.241	−0.0069	−0.0066	−0.0064
0.251	−0.3630	−0.1575	−0.1460	−0.1194	0.244	0.0074	0.0062	0.0034
0.257	−0.3624	−0.0546	−0.0504	−0.0415	0.254	0.0770	0.0687	0.0516
0.260	−0.3621	0.0000	0.0000	0.0000	0.260	0.1495	0.1341	0.1022

$r_u = 300$ in., $f = 576$ in., $\nu = 0.3$, $h = 1$ in.

Mem. = Membrane, S.S. = Shallow Shell

A.I. = Asymptotic Integration, N.I. = Numerical Integration

show a very close agreement among the stress resultants and the bending moments obtained by the different methods of analysis (Figures 5, 6, 7, and 8; Tables I, II, and III). The larger discrepancies in the tangential and normal displacement components have been explained in a previous section.

As concluded qualitatively in previous investigations, the membrane behavior is indeed the dominant behavior of the shell except for an edge zone of width d (for the type of loading and boundary conditions considered here). Since we consider only shells for which

$$\frac{(2f)^2\rho_0}{Eh} \ll 1 \tag{25}$$

deviations from linear membrane theory are effectively due to bending [10] and the edge zone width is indeed of the order $(2fh)^{1/2}$

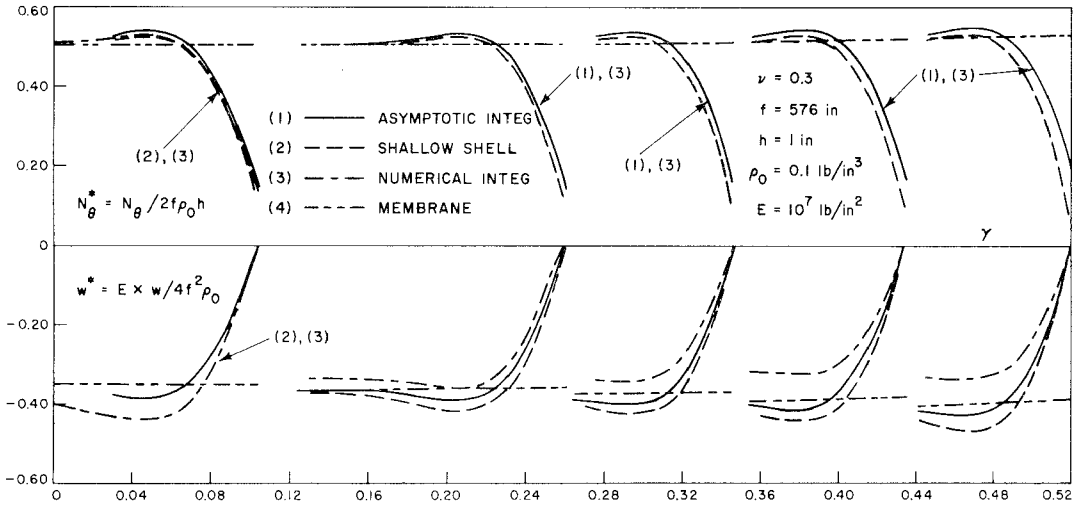

Figure 5. Comparison of solutions for various size shells.

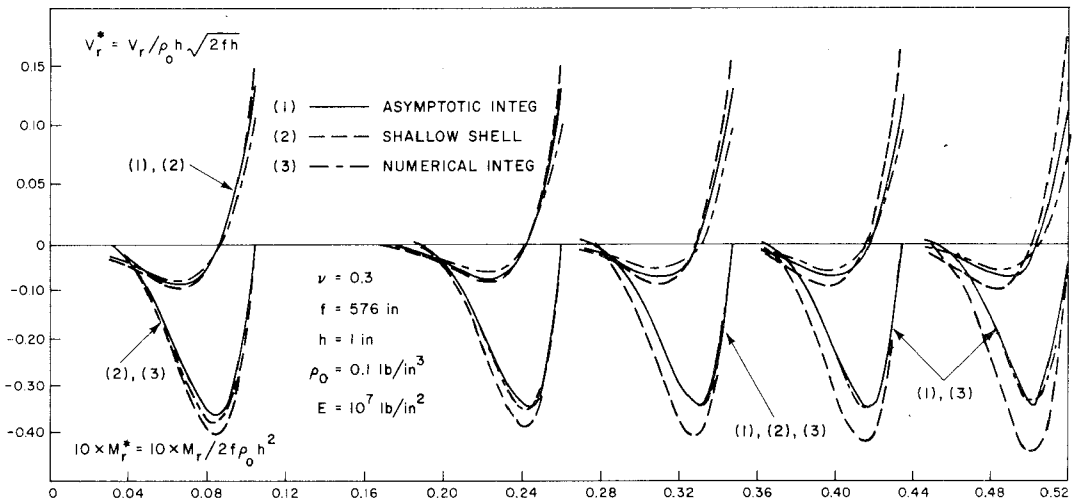

Figure 6. Comparison of solutions for various size shells.

(Figures 3 and 4) [9]. Note that if the inequality (25) is violated, then the nonlinear membrane action must also be considered [11], [12]. Figures 5 and 6 show that d is practically independent of r_u for $\gamma_u < 1$.

$$d \cong 2\sqrt{2fh} \tag{26}$$

As a result, the approximation of the shell behavior by membrane behavior becomes increasingly crude as $\gamma_u \to 0$ if f and h are kept fixed (Figure 5). In particular, the membrane analysis of shells invariably predicts a maximum normal displacement at the apex of the shell while other analyses show that as $\gamma_u \to 0$, w_{max} moves away from the apex toward the edge of the shell.

For a fixed r_u, calculations show that all the starred quantities in (27) are independent of E and ρ_0. A change in f or h (again keeping r_u fixed) affects both the edge zone width (in a manner already described) and the amplitude of these quantities (N_r^*, N_θ^*, w_r^* increase while M_r^*, M_θ^*, V_r^*, and θ_r^* decrease as f or h increases). However, the effect on the amplitudes is not appreciable (percentagewise), even if the change in γ_u is large, so long as $\gamma_u \leq 0.8$. Fixing f and h while varying r_u clearly results again in variations on the amplitudes in the same manner as keeping r_u and h fixed while varying f. For $\gamma_u \leq 0.8$, the change in the amplitude of all these quantities is again not appreciable even for a large variation in γ_u (Figures 5 and 6). This latter observation is particularly important in the design of large antennae for the obvious reason. It is interesting to observe also that, except for the usual narrow edge zone, the deformation induced by gravity is independent of the shell thick-

Table II: **Comparison of Results**

$10 \times M_r^* = 10 \times M_r/2f\rho_0 h^2$ | $10 \times M_\theta^* = 10 \times M_\theta/2f\rho_0 h^2$

γ	Mem.	S.S.	A.I.	N.I.	Mem.	S.S.	A.I.	N.I.
0.397		0.0062	0.0020	0.0020		0.0024	0.0003	0.0003
0.404		0.0093	0.0041	0.0041		0.0034	0.0010	0.0010
0.417		0.0167	0.0096	0.0096		0.0060	0.0026	0.0028
0.430		0.0215	0.0149	0.0145		0.0079	0.0043	0.0045
0.443		0.0135	0.0133	0.0123		0.0060	0.0037	0.0042
0.449		−0.0005	0.0060	0.0047		0.0019	0.0016	0.0020
0.462		−0.0614	−0.0329	−0.0346		−0.0172	−0.0102	−0.0101
0.475		−0.1779	−0.1171	−0.1191		−0.0550	−0.0354	−0.0366
0.488		−0.3357	−0.2424	−0.2436		−0.1085	−0.0729	−0.0773
0.501		−0.4456	−0.3423	−0.3426		−0.1506	−0.1030	−0.1122
0.508		−0.4205	−0.3312	−0.3313		−0.1480	−0.0996	−0.1117
0.514		−0.2892	−0.2327	−0.2328		−0.1124	−0.0701	−0.0846

$N_r^* = N_r/2f\rho_0 h$ | $N_\theta^* = N_\theta/2f\rho_0 h$

γ	Mem.	S.S.	A.I.	N.I.	Mem.	S.S.	A.I.	N.I.
0.039	0.5006	0.5000	0.5006	0.5006	0.5002	0.5000	0.5002	0.5002
0.202	0.5152	0.5000	0.5152	0.5152	0.5049	0.5000	0.5049	0.5049
0.306	0.5349	0.5000	0.5349	0.5349	0.5109	0.5001	0.5109	0.5109
0.365	0.5495	0.5000	0.5495	0.5495	0.5150	0.4995	0.5147	0.5147
0.410	0.5626	0.4999	0.5625	0.5625	0.5185	0.4996	0.5176	0.5177
0.449	0.5749	0.5006	0.5752	0.5751	0.5216	0.5211	0.5354	0.5355
0.469	0.5815	0.5017	0.5826	0.5823	0.5232	0.5310	0.5479	0.5473
0.488	0.5884	0.5022	0.5900	0.5897	0.5249	0.4824	0.5194	0.5180
0.508	0.5955	0.4983	0.5944	0.5948	0.5266	0.2825	0.3675	0.3659
0.521	0.6004	0.4901	0.5932	0.5951	0.5277	0.0521	0.1801	0.1785

$w^* = Ew/4f^2\rho_0$ | $V_r^* = V_r/\rho_0 h\sqrt{2fh}$

γ	Mem.	S.S.	A.I.	N.I.	γ	S.S.	A.I.	N.I.
0.039	−0.4492	−0.3634	−0.4492	−0.3484	0.391	0.0010	0.0005	0.0004
0.208	−0.4407	−0.3781	−0.4407	−0.3419	0.410	0.0018	0.0012	0.0009
0.332	−0.4269	−0.4015	−0.4270	−0.3312	0.430	0.0003	0.0008	0.0006
0.417	−0.4135	−0.4245	−0.4132	−0.3202	0.436	−0.0016	−0.0002	−0.0001
0.443	−0.4086	−0.4473	−0.4189	−0.3423	0.456	−0.0137	−0.0079	−0.0059
0.469	−0.4034	−0.4725	−0.4306	−0.3330	0.469	−0.0270	−0.0175	−0.0133
0.488	−0.3993	−0.4310	−0.3932	−0.3043	0.482	−0.0375	−0.0266	−0.0204
0.501	−0.3964	−0.3222	−0.2967	−0.2304	0.501	−0.0077	−0.0088	−0.0079
0.514	−0.3934	−0.1241	−0.1153	−0.0902	0.508	0.0302	0.0183	0.0121
0.521	−0.3919	0.0000	0.0000	0.0000	0.521	0.1754	0.1274	0.0943

r_u = 600 in., f = 576 in., ν = 0.3, h = 1 in.
Mem. = Membrane, S.S. = Shallow Shell
A.I. = Asymptotic Integration, N.I. = Numerical Integration

ness while, if $\gamma_u \leq 0.8$, the variations of the displacements as a function of the thickness in this edge zone are negligibly small. The same can be said of the maximum stresses $(\sigma_r)_{max}$ and $(\sigma_\theta)_{max}$ as seen from the following relations.

$$(\sigma_r)_{\max} = \frac{N_r}{h} + \frac{6(M_r)_{\max}}{h^2} = 2f\rho_0 [N_r^* + 6(M_r^*)_{\max}]$$

$$(\sigma_\theta)_{\max} = \frac{N_\theta}{h} + \frac{6(M_\theta)_{\max}}{h^2} = 2f\rho_0 [N_\theta^* + 6(M_\theta^*)_{\max}] \quad (28)$$

While no presentation of this nature can tabulate all the results needed for design purposes and give exhaustive discussion of these results, an attempt has been made here to treat a typical shell which exhibits most

Table III: **Comparison of Results**

$10 \times M_r^* = 10 \times M_r/2f\rho_0 h^2$ | $10 \times M_\theta^* = 10 \times M_\theta/2f\rho_0 h^2$

γ	Mem.	S.S.	A.I.	N.I.	Mem.	S.S.	A.I.	N.I.
0.850			−0.0010	−0.0010			−0.0005	−0.0007
0.863			−0.0011	−0.0010			−0.0006	−0.0007
0.875			−0.0007	−0.0004			−0.0004	−0.0005
0.888			0.0011	0.0012			0.0001	0.0001
0.900			0.0050	0.0044			0.0012	0.0012
0.913			0.0104	0.0084			0.0029	0.0027
0.925			0.0132	0.0095			0.0037	0.0032
0.938			0.0025	−0.0022			0.0005	−0.0007
0.950			−0.0399	−0.0426			−0.0122	−0.0149
0.963			−0.1301	−0.1265			−0.0392	−0.0446
0.975			−0.2523	−0.2402			−0.0759	−0.0857
0.988			−0.2992	−0.2847			−0.0900	−0.1041

$N_r^* = N_r/2f\rho_0 h$ | $N_\theta^* = N_\theta/2f\rho_0 h$

γ	Mem.	S.S.	A.I.	N.I.	Mem.	S.S.	A.I.	N.I.
0.075	0.5021		0.5021	0.5021	0.5007		0.5007	0.5007
0.500	0.5924		0.5924	0.5926	0.5259		0.5259	0.5259
0.625	0.6438		0.6438	0.6439	0.5369		0.5369	0.5370
0.725	0.6926		0.6926	0.6927	0.5459		0.5459	0.5459
0.800	0.7337		0.7337	0.7338	0.5525		0.5525	0.5525
0.888	0.7865		0.7865	0.7866	0.5600		0.5591	0.5593
0.950	0.8274		0.8277	0.8276	0.5651		0.5856	0.5829
0.975	0.8444		0.8450	0.8449	0.5671		0.5434	0.5401
0.988	0.8531		0.8528	0.8530	0.5681		0.4375	0.4371
1.000	0.8619		0.8589	0.8600	0.5690		0.2586	0.2580

$w^* = Ew/4f^2\rho_0$ | $V_r^* = V_r/\rho_0 h\sqrt{2fh}$

γ	Mem.	S.S.	A.I.	N.I.	γ	S.S.	A.I.	N.I.
0.075	−0.7876		−0.7876	−0.6400	0.888		0.0005	0.0003
0.349	−0.7456		−0.7456	−0.6042	0.900		0.0009	0.0005
0.575	−0.6733		−0.6733	−0.5434	0.913		0.0009	0.0005
0.738	−0.6002		−0.6002	−0.4796	0.925		−0.0002	−0.0002
0.813	−0.5600		−0.5600	−0.4437	0.938		−0.0039	−0.0028
0.875	−0.5230		−0.5222	−0.4099	0.950		−0.0111	−0.0078
0.925	−0.4911		−0.4982	−0.3866	0.963		−0.0195	−0.0140
0.950	−0.4744		−0.5027	−0.3845	0.975		−0.0196	−0.0154
0.988	−0.4481		−0.2647	−0.2028	0.988		0.0104	0.0033
1.000	−0.4391		0.0000	0.0000	1.000		0.1016	0.0675

r_u = 1152 in., f = 576 in., ν = 0.3, h = 1 in.

Mem. = Membrane, S.S. = Shallow Shell

A.I. = Asymptotic Integration, N.I. = Numerical Integration

of the shell characteristics and to discuss some of the interesting observations. Other aspects of a paraboloidal shell of revolution can be found in [1], and, if necessary, in the computer programs which generate the needed information. In this same reference, the problem of a shell oriented arbitrarily with respect to the direction of gravity was also treated.

ACKNOWLEDGEMENT

The authors gratefully acknowledge the invaluable aid of Miss Elaine Boyce in the preparation of this paper.

REFERENCES

[1] J. W. Mar and F. Y. M. Wan. "Distortions and Stresses of Paraboloidal Surface Structures," parts II-V, *Lincoln Laboratory Report 71G-1*, February 1962.

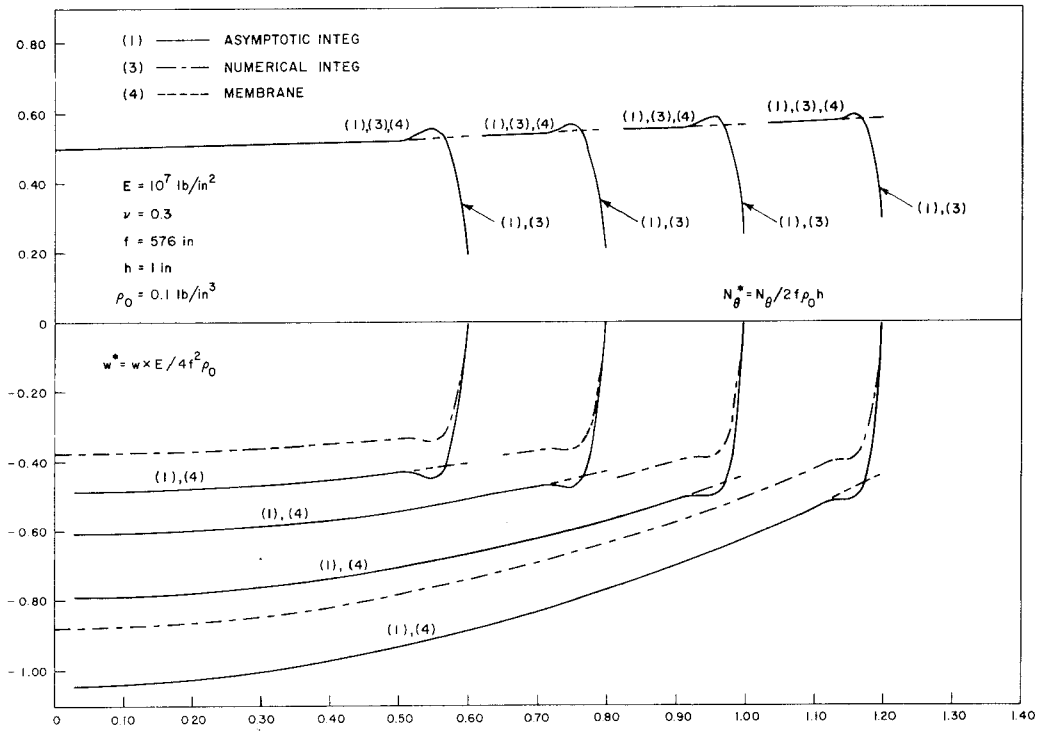

Figure 7. Comparison of solutions for various size shells.

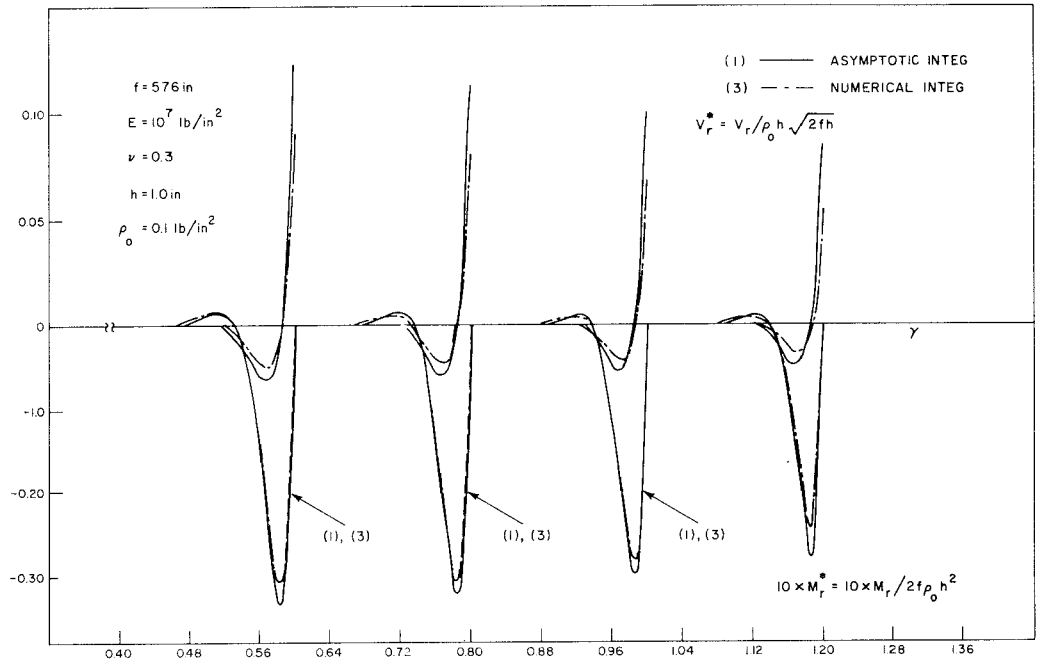

Figure 8. Comparison of solutions for various size shells.

[2] V. V. Novozhilov. *The Theory of Thin Shells,* P. Noordhoff Ltd., Groningen-The Netherlands, 1959.

[3] E. Reissner. "A Note on Membrane and Bending Stresses in Spherical Shells," *J. Soc. Indust. Appl. Math.*, Vol. 4, No. 4, December 1956, pp. 230-240.

[4] K. Marguerre. "Zur Theorie der gekrümmten Platte grosser Formänderung," *Proc. 5th Intern. Congr. Appl. Mechanics,* 1938, pp. 93-101.

[5] E. Reissner. "Stresses and Small Displacements of Shallow Spherical Shells, II," *J. of Math. and Phys.*, Vol. 25, 1946, pp. 279-300; Vol. 27, p. 240.

[6] E. Meissner. "Das Elastizitätsproblem für

dünne Schalen von Ringflächen-Kugen-oder Kegelform," *Physikalische Zeitschrift,* Vol. 14, 1913, p. 343.
[7] E. Meissner. "Über Elastizität und Festigkeit dünner Schalen," *Vierteljahrschrift der Naturforschenden Gesellschaft in Zürich,* Vol. 60, 1915, p. 23.
[8] F. B. Hildebrand. "On Asymptotic Integration in Shell Theory," *Proceedings of Symposia in Applied Mathematics,* Vol. III, 1949, pp. 53-66.
[9] W. H. Wittrick. "Edge Stresses in Thin Shells of Revolution," *Melbourne Aeronautical Research Lab., Report SM-253,* 1957.
[10] H. Reissner. *Spannungen in Kugel-shalen (Kuppeln),* Müller-Breslan Festschrift, 1912, pp. 181-193.
[11] E. Bromberg and J. J. Stoker. "Non-linear Theory of Curved Elastic Sheets," *Quarterly of Appl. Math.,* Vol. 3, 1945, pp. 246-265.
[12] E. Reissner. "The Edge Effect in Symmetric Bending of Shallow Shells of Revolution," *Communications of Pure and Applied Mathematics,* Vol. XII, 1959, pp. 385-398.
[13] C. N. DeSilva. "Deformation of Elastic Paraboloidal Shells of Revolution," *Journal of Applied Mechanics,* Vol. 24, 1957, pp. 397-404.

SUPPLEMENTARY NOTATION

y^1, y^2, y^3	rectangular coordinates
f	focal length of the paraboloid
r	radius of revolution of the paraboloidal surface
$\vec{a}_1, \vec{a}_2$	covariant base vectors of the middle surface of the undeformed shell
$\vec{n}$	inward normal to the middle surface of the undeformed shell
γ	slope of the meridional tangent to the paraboloidal surface
φ	angle between the meridional tangent and the tangent plane to the apex of the paraboloidal surface
ρ_0	weight density (force per unit volume)
A	$\frac{1}{Eh}$
r_u	the upper edge of the shell
r_l	the lower edge of the shell
$C_1, C_2, \ldots C_6$	constants of integration
$K_1, K_2, \ldots K_6$	constants of integration